

Yury KAMENIR\* and Giuseppe MORABITO<sup>1)</sup>

The Mina & Everard Goodman Faculty of Life Sciences, Bar-Ilan University, Ramat-Gan 52900, Israel

<sup>1)</sup>CNR Istituto per lo Studio degli Ecosistemi, L.go Tonolli 50-52, 28922 Verbania-Pallanza, Italy

\*email corresponding author: [kamenir@mail.biu.ac.il](mailto:kamenir@mail.biu.ac.il)

---

## ABSTRACT

Due to the rapid and common deterioration of aquatic ecosystems, scientists and environmental protection organizations acutely need means capable of producing quantitative estimates for structural deformations of natural communities. Recently, very common biomass size spectra ignore community taxonomic composition, i.e., one of the most important kinds of biological information. Therefore, another very old, but rare in planktonology, method – the traditional taxonomic size spectrum (TTSS) – can be helpful. TTSS, a specific form of size-frequency distribution of taxonomic units, reveals repeating patterns of deep subalpine Lago Maggiore (Italy) phytoplankton taxonomic structure. The general TTSS pattern was safeguarded during 22 annual cycles (1984-2005), when many principal environmental characteristics were changed considerably during the lake oligotrophication. At the same time, the fine structure deformations of this pattern helped us divide the total oligotrophication process into several stages characterized by notable changes of TTSS peaks' proportions. These peak-height alterations were caused by pronounced changes in the species list and overall taxonomic diversity of the lake phytoplankton. The average cell volume decline was found. It was significantly correlated with the total phosphorus descending trend. This cell volume decline was produced by the addition of numerous species into the medium-and-small size fractions. Typical patterns of the stable and transitory stages were differentiated, which could be valuable for environmental protection and diagnostic applications. The central peak height difference between the stable and the transitory periods was statistically significant. Oligotrophication process decomposition into several more homogenous groups of years was supported by quantitative estimators produced by hierarchical cluster analysis. The highest level of the similarity measure (Pearson  $r$ ) in pairs of annual TTSS was close to the respective estimates found for other lakes. Concomitantly, its minimal level, produced by a specific pair of abnormal years at the beginning and end of the studied process, was found previously only for pairs taken from two different ecosystems (Lakes Kinneret and Tahoe). This way, TTSS can be applied as a quantitative analysis means of the integral natural community structural evolution. Such tools are acutely needed for environmental management, monitoring, and theoretical ecology.

Key words: community structure stability, size-frequency distribution, anthropogenic impact

---

## 1. INTRODUCTION

It is a common concern that our aquatic ecosystems deteriorate due to numerous and ever-growing anthropogenic impacts. For this reason, ecologists try to find means for quantitative estimations of structural deformation for natural communities (Odum 1971; Begon *et al.* 1996). Size spectrum analysis (Sheldon *et al.* 1972; Sprules & Munawar 1986) is one of the tools available to characterize the whole community structure. The 'ataxonomic' biomass size spectrum (BSS) and normalized biomass size spectrum (NBS) are closely connected to a more traditional one, where the size-frequency distribution of species or higher taxa is plotted (Hemmingsen 1934; Hutchinson & MacArthur 1959; Smith *et al.* 2004). While, in some important cases, not all registered taxonomic units are determined and described at the species level, we apply the operational taxonomic unit (OTU) approach (Sneath & Sokal 1973), and refer to such size distribution of taxonomic units as traditional taxonomic size spectrum (TTSS; Kamenir *et al.* 2006).

Like the NBS, the species size-distribution patterns observed for pelagic and benthic assemblages seem to be rather stable even during pronounced changes in community composition (Havlicek & Carpenter 2001; Kamenir *et al.* 2006). At the same time, changes of the TTSS fine structure are often evident. Therefore, comparisons of statistical distributions of species can produce quantitative similarity or distance measures estimating the change in the community composition between two points in time (Thibault *et al.* 2004; Kamenir *et al.* 2006). Consequently, TTSS, a simple and flexible presentation of an important property of the community (i.e., its taxonomic composition), seems to be a promising tool needed for ecological monitoring, forecasts, and quantitative assessments of the aquatic assemblage structural deformations. The interesting and valuable phenomenon (for many theoretical and applied applications) of long-term consistency of the general pattern of phytoplankton TTSS was initially established for one lake (Kinneret; Kamenir *et al.* 2006). The following studies (Kamenir *et al.* 2008) have supported its more general nature, including oligotrophic lake condi-

tions. Thus, it seems that the phytoplankton TTSS pattern is likely to be supported by some ecological mechanisms of a very general nature and demands further studies considering specific objects and situations of general ecological interest (Kamenir *et al.* 2008). The high self-similarity of the TTSS general pattern during long-term (>20 years) periods can be interpreted as the strength of the ecological community self-maintenance. The role of specific anthropogenic and natural impacts – such as lake size, depth, and trophic status change – seems to be very interesting and important, especially during times of global change.

In this study, we applied the TTSS approach to analyze structural changes of the phytoplankton assemblage in the deep subalpine Lago Maggiore (Italy) during a long period of time. We chose Lago Maggiore as a case study because a clear and thoroughly documented oligotrophication process took place there (e.g., Salmaso *et al.* 2007), and a multi-annual phytoplankton record was available describing the concurrent phytoplankton change.

The objective of our study was to examine the TTSS pattern change of the Lago Maggiore phytoplankton assemblage during a thoroughly documented oligotrophication process. We examined if typical patterns of the assemblage structure can be established. Then we tried to establish specific trends and break down the total 22-year range into several shorter periods of more homogeneous (i.e., self-similar) patterns.

The working hypothesis was that repeating annual succession patterns are produced by communities that preserve some reliable structural features. This reliability can decline during the years of pronounced changes of the ecosystem state, caused by nutrient-level decline. Different typical patterns may exist during the stable and transitory stages.

## 2. METHODS

### 2.1. Long-term oligotrophication process of Lago Maggiore

Lago Maggiore, the second largest subalpine lake in Italy (lake area of 213 km<sup>2</sup>, drainage area of 6599 km<sup>2</sup>), is situated at 193 m above mean sea level. It has a maximum depth of 370 m and an average depth of 178 m, as reported in Salmaso *et al.* (2007). It is oligotrophic by nature, as shown by early limnological studies (Baldi 1949) and by analysis of the sedimentary pigments (Guilizzoni *et al.* 1983). The eutrophication process started in the sixties: the nutrient concentration (phosphorus) in the lake water began to rise and was soon followed by an increase in phytoplankton abundance, biovolume, and primary production (Ravera & Vollenweider 1968; Morabito & Pugnetti 2000).

In the late seventies, the lake reached a trophic state close to eutrophy, when the P loads peaked and the maximum in-lake TP concentration was recorded (around 30 µg L<sup>-1</sup> at winter mixing; Mosello & Ruggiu

1985). Since that time, the P loads have been gradually reduced by various means, including the establishment of sewage treatment plants and the reduction of total phosphorus in detergents. As a result, the TP values have gradually decreased to some 10 µg L<sup>-1</sup> (Ruggiu *et al.* 1998). The slow reversal of the trophic state of Lago Maggiore is documented in many papers.

In the eighties, strong emphasis was put on the apparent resilience of the plankton communities against falling levels of phosphorus (de Bernardi *et al.* 1988). However, starting from 1987-88, major biological changes were at last manifested, especially in the phytoplankton (Manca *et al.* 1992). Among the recorded alterations, a remarkable decrease in average cell size and increased importance of the smaller size phytoplankters were notable (Ruggiu *et al.* 1998).

### 2.2. Data sampling and treatment

Water samples were collected for phytoplankton analysis fortnightly, but monthly during the cold months (November to January), at the station of Ghiffa, corresponding to the deepest point of the lake. A bottle, designed to take an integrated sample in the 0-20 m water layer, was used. The bottle was home-made at Institute for Ecosystem Studies (R. Bertoni, 1996; Patent. Num. MI 96/A 000121). Its main body is a plastic cylinder, into which a piston is placed. A cable 20 meters length is connected to the piston through a wheel and the piston moves when the bottle is sinking into the water. The device allows a continuous sampling from the water column, taking a fixed volume of water at each meter. Phytoplankton was determined in subsamples of 10 mL preserved in acetic Lugol's solution. Algal cells were identified and measured on a Zeiss Axiovert 10 microscope, following Lund *et al.* (1958), until 400 cells of the most important species were counted. Algae >2 µm in GALD (Greatest Axial Linear Dimension) were classified and included into our analysis. Algae up to some 1 µm in GALD were classified among the small Chroococcales when in colonies, whereas single cells were included among unidentified picoplankton. Due to the difficulties in quantifying properly this category with the counting method used, picoplankton was not included in the current analysis.

For determination of the phytoplankton species the standard systematic literature was used. Oscillatoriales were determined also following Anagnostidis & Komárek (1988). Water for chemical analyses was collected monthly and nutrient concentrations were determined at the chemical laboratory of the Istituto per lo Studio degli Ecosistemi (Pallanza), following the methods reported in Mosello & Ruggiu (1985). These procedures of data sampling and processing were very similar to protocols followed up at Lake Kinneret [described in detail in Zohary (2004)], where TTSS long-term consistency was originally found (Kamenir *et al.* 2006).

### 2.3. Operational taxonomic units and taxonomic size spectra

A mean biovolume of the individual cell of each species was calculated from linear microscope measurements and the closest geometrical shape (Hillebrand *et al.* 1999). This cell volume was the parameter used for allocating a taxon to a size class. Size classes were created by doubling the cell volume, i.e., by standard increments of the cell size logarithm. Thus, our size classes were  $\leq 0.5 \mu\text{m}^3$ , followed by 0.5-1, 1-2, 2-4  $\mu\text{m}^3$ , etc., up to the largest phytoplankton cell of 85,180  $\mu\text{m}^3$  (*Peridinium williei*). The  $\log V_{xx}$  notation is used throughout this paper for size classes, where xx is the logarithm of the class right boundary,  $\log_{10}(V)$ .

Since not all our taxa were strictly identified species, we refer to each as an operational taxonomic unit, or OTUj (Sneath & Sokal 1973). Throughout the 22 years of analysis, the phytoplankton assemblages of L. Maggiore were made up by >200 taxonomic units. For each OTUj, an annual average volume ( $V_j$ ) was applied. This volume ( $V_j$ ) was obtained by measuring at least 50 single algal cells and using the arithmetic mean of the 50 measurements for each geometrical dimension. As a rule, these 50 measurements were taken throughout the whole year, randomly, from the different seasonal samples; however, for species characterized with a pronounced seasonality (e.g., spring months for diatoms), they were taken during the respective period.

For those species regularly occurring during the time period analyzed, the volume estimate was checked throughout the years. It was measured many times by randomly checking its geometric dimensions on some specimens. If a significant (>10%) change of  $V_j$  was supposed, a more thorough procedure was carried out. If a size shift was evident, allocating the species annual mean into another size class, it was registered as a new (different) OTUj of the same species (see table 2 in Appendix).

The average of the log-transformed cell volume estimates of all species, comprising the annual list of species, was calculated. It was transformed back and applied as the annual average cell volume. Twenty-two traditional taxonomic size spectra, describing period from 1984 to 2005, were created for L. Maggiore phytoplankton, one for each year. A TTSS was created as the frequency distribution (histogram) of the total number of OTUj-s registered during one year to size classes. The histograms were built using the Histogram and Crosstabs procedures of the statistical package SPSS, and assigned according to the year they represented. LMttXX notation was applied, where XX was the year, for example LMtt98 was the TTSS for year 1998 (Kamenir *et al.* 2006).

### 2.4. Statistical analysis

Hierarchical cluster analysis was applied to estimate the measure of similarity between histograms and to pull together the most similar TTSS shapes. Each histo-

gram, i.e., a column of numbers, was interpreted as a numerical vector (Cha & Srihari 2002). The Pearson correlation was applied to estimate the similarity (Sneath & Sokal 1973). One-way ANOVA with Bonferroni post-test was performed to compare the annual OTUj number for several groups of years, differentiated by hierarchical cluster analysis (see below). The dynamics of each size fraction was described by its OTUj number registered per year. The curve-fitting (linear) model was used to calculate parameters of linear regressions of the inter-annual dynamics curves. SPSS program, version 14.0, was used for all statistical procedures.

## 3. RESULTS

The 22 annual TTSSs, compared in graphic form, show variable shapes; however, the same general pattern is seen while comparing all 22 TTSS (Fig. 1). This pattern represents several modes of more-or-less the same height within the size (LogV) range of 1 to 4, with much lower peaks in both peripheral zones. In reality, one can see several peaks divided by rather deep troughs. The number of peaks and their positions slightly vary at times. With the help of hierarchical cluster analysis, this set of shapes was divided into several subclusters or periods characterized with higher homogeneity (Fig. 2; Tab. 1). Then we can see almost the same shape of four central peaks (region  $\text{LogV}=1-4$ ) with much lower peripheral bells at  $\text{LogV}=0.0-0.9$  and  $\text{LogV}=4.2-5.1$  (Fig. 3). During the first period (1984-1987), the central region strongly resembled a symmetrical Gaussian bell (Fig. 3A). During the second period (1988-1991), the second-from-the-left main peak (V2.4) drastically changed and became the sole dominant (Fig. 3B). In reality, this change, clearly seen during the numerous following years (Fig. 3B-D), is evident already while comparing years 1985 and 1986 (Fig. 3A). A trough at V2.7 was already clearly seen in 1986 (Fig. 3A), dividing the central bell of 1985 into two peaks, at V2.4 and V3.0; but the apparent later peak at V2.4 was still overshadowed (until 1988) by peak V3.0 (Fig. 3 A-B).

During the next period, this peak rose up, then diminished for one year in 1991 (Fig. 3B-C), and again became dominant till 2002 (Figs. 3E-F). Thanks to this peak (V2.4), we see a long period of TTSS-shape homogeneity (1990-2001) that was very different from the previous and following years (Figs 2 and 3F; Tab. 1). After 2001, this peak again drastically diminished and was overshadowed by its neighbor on the left at V2.1 (Fig. 3E). This dynamics of one peak, experiencing pronounced risings and fallings, creates a visual impression of the peak side shift (Figs 3E and F). Analogous drastic changes are notable for peaks at V1.8 in 1999 and V3.0 in 2003 (Fig. 1). They can also be seen for the peripheral zones ( $\text{LogV}<1$  and  $\text{LogV}>4$ ), but catch less attention due to the small changes of the peripheral peaks, being produced by addition/deletion of only 1-2 species (Fig. 1).

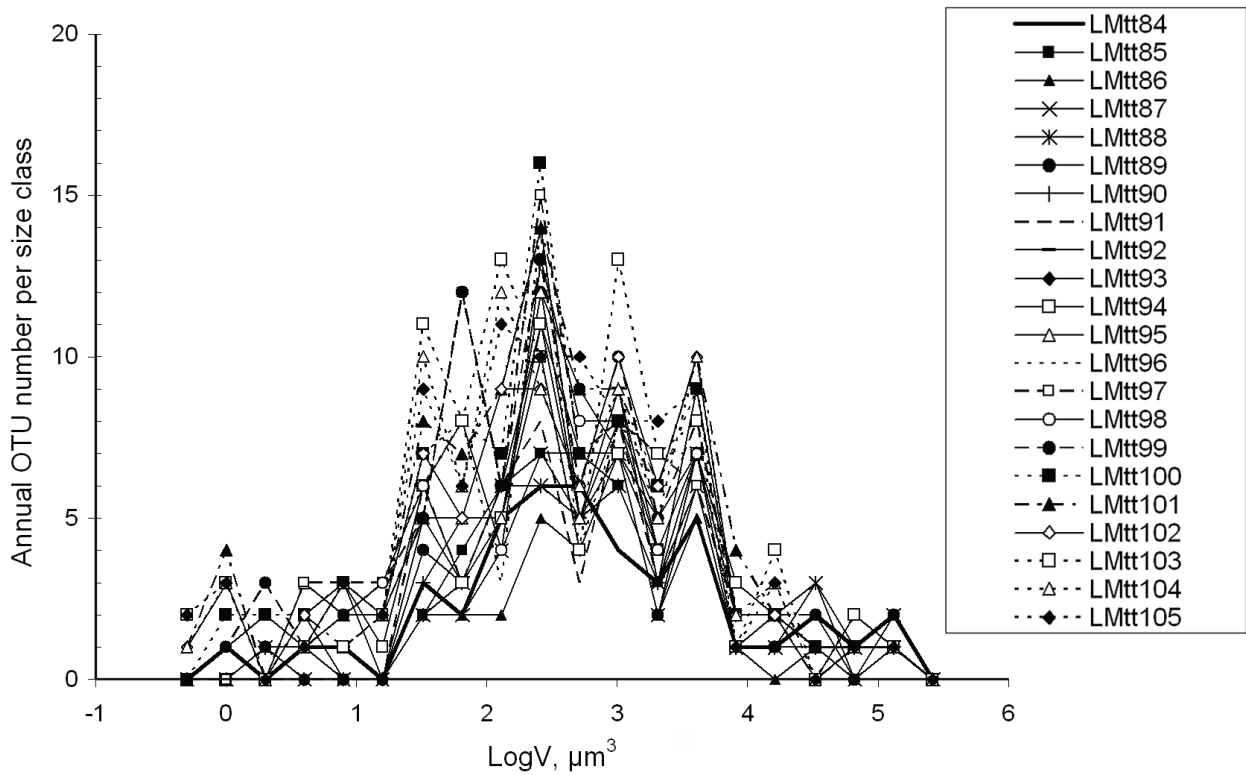


**Fig. 1.** Annual taxonomic size spectrum (TTSS) of phytoplankton during 22 consecutive years of Lago Maggiore (Italy) oligotrophication process. Each TTSS (LMttXX) was created as the frequency distribution (histogram) of the cumulative number of OTUs registered during one year to size classes, according to the mean annual cell volume estimate ( $V, \mu\text{m}^3$ ) of each OTU<sub>j</sub> (see Methods). XX describe the year number, from 1984 to 1999 and 2000 to 2005; OTU<sub>j</sub> is operational taxonomic unit.

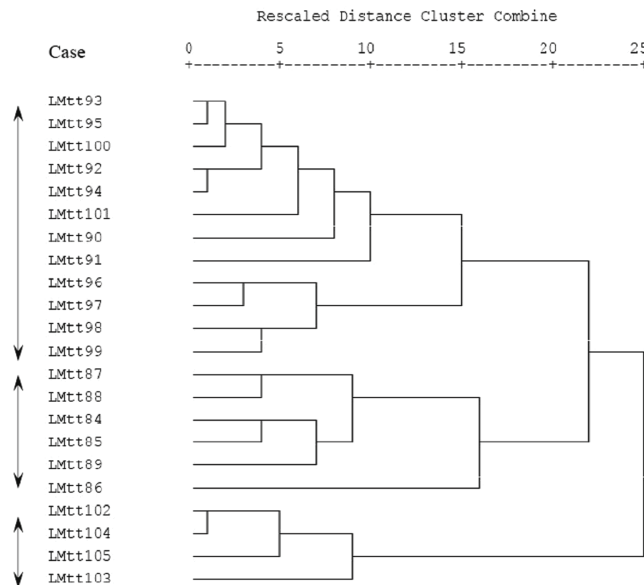


**Fig. 2.** The hierarchical cluster analysis decomposition (dendrogram) of the total oligotrophication period (1984-2005) into subclusters of less heterogeneous taxonomic size structure of L. Maggiore phytoplankton. Three vertical arrows delimit three main subclusters (1990-2001, 1984-1989, and 2002-2005). For the secondary-level sub-clusters see also the proximity matrix (Tab. 1). The Pearson correlation coefficient ( $r$ ) was applied as the measure estimating similarity between size spectra considered as numerical vectors. Even for time intervals up to 20 years,  $r > 0.66$ , and mostly,  $r > 0.8$  (Tab. 1). The proximity values are rescaled to the respective distances by the SPSS program.



**Tab. 1.** Proximity matrix for the cluster analysis results (dendrogram, Fig. 2). Pearson  $r$  is applied as the similarity measure;  $r > 0.66$  for all pairs of years. High similarities ( $r > 0.9$ ) are highlighted. The borders delimit homogenous time-intervals (each  $r > 0.9$ ). Dashed borders denote a high similarity between two distant blocks (years 1992-1995 and 2000-2001).

Case	LMtt 84	LMtt 85	LMtt 86	LMtt 87	LMtt 88	LMtt 89	LMtt 90	LMtt 91	LMtt 92	LMtt 93	LMtt 94	LMtt 95	LMtt 96	LMtt 97	LMtt 98	LMtt 99	LMtt 100	LMtt 101	LMtt 102	LMtt 103	LMtt 104	LMtt 105
LMtt84		0.943	0.815	0.890	0.918	0.933	0.865	0.835	0.879	0.845	0.899	0.834	0.697	0.727	0.788	0.723	0.836	0.887	0.849	0.712	0.812	0.884
LMtt85	0.943		0.859	0.898	0.931	0.919	0.904	0.832	0.892	0.858	0.875	0.877	0.757	0.815	0.841	0.831	0.860	0.905	0.873	0.752	0.811	0.869
LMtt86	0.815	0.859		0.921	0.867	0.869	0.835	0.841	0.883	0.816	0.824	0.834	0.739	0.686	0.799	0.782	0.770	0.788	0.805	0.678	0.680	0.688
LMtt87	0.890	0.898	0.921		0.944	0.934	0.907	0.885	0.909	0.838	0.860	0.840	0.718	0.694	0.787	0.776	0.804	0.811	0.800	0.691	0.724	0.735
LMtt88	0.918	0.931	0.867	0.944		0.885	0.914	0.880	0.882	0.842	0.830	0.815	0.687	0.704	0.760	0.787	0.805	0.837	0.854	0.752	0.804	0.812
LMtt89	0.933	0.919	0.869	0.934	0.885		0.912	0.847	0.913	0.859	0.931	0.884	0.781	0.786	0.894	0.812	0.895	0.893	0.797	0.669	0.743	0.805
LMtt90	0.865	0.904	0.835	0.907	0.914	0.912		0.915	0.954	0.920	0.896	0.921	0.825	0.826	0.869	0.879	0.923	0.911	0.871	0.804	0.828	0.807
LMtt91	0.835	0.832	0.841	0.885	0.880	0.847	0.915		0.961	0.916	0.894	0.891	0.800	0.746	0.808	0.810	0.857	0.885	0.901	0.902	0.891	0.829
LMtt92	0.879	0.892	0.883	0.909	0.882	0.913	0.954	0.961		0.957	0.961	0.957	0.862	0.816	0.877	0.844	0.918	0.930	0.909	0.830	0.849	0.838
LMtt93	0.845	0.858	0.816	0.838	0.842	0.859	0.920	0.916	0.957		0.949	0.966	0.924	0.893	0.900	0.899	0.955	0.916	0.908	0.826	0.854	0.855
LMtt94	0.899	0.875	0.824	0.860	0.830	0.931	0.896	0.894	0.961	0.949		0.948	0.862	0.829	0.909	0.817	0.932	0.929	0.881	0.751	0.832	0.864
LMtt95	0.834	0.877	0.834	0.840	0.815	0.884	0.921	0.891	0.957	0.966	0.948		0.958	0.919	0.929	0.895	0.963	0.923	0.882	0.791	0.806	0.822
LMtt96	0.697	0.757	0.739	0.718	0.687	0.781	0.825	0.800	0.862	0.924	0.862	0.958		0.948	0.920	0.906	0.938	0.853	0.783	0.723	0.700	0.728
LMtt97	0.727	0.815	0.686	0.694	0.704	0.786	0.826	0.746	0.816	0.893	0.829	0.919	0.948		0.930	0.946	0.933	0.854	0.762	0.720	0.707	0.764
LMtt98	0.788	0.841	0.799	0.787	0.760	0.894	0.869	0.808	0.877	0.900	0.909	0.929	0.920	0.930		0.943	0.958	0.910	0.809	0.727	0.754	0.802
LMtt99	0.723	0.831	0.782	0.776	0.787	0.812	0.879	0.810	0.844	0.899	0.817	0.895	0.906	0.946	0.943		0.932	0.865	0.808	0.776	0.758	0.761
LMtt100	0.836	0.860	0.770	0.804	0.805	0.895	0.923	0.857	0.918	0.955	0.932	0.963	0.938	0.933	0.958	0.932		0.945	0.869	0.783	0.824	0.851
LMtt101	0.887	0.905	0.788	0.811	0.837	0.893	0.911	0.885	0.930	0.916	0.929	0.923	0.853	0.854	0.910	0.865	0.945		0.934	0.845	0.902	0.923
LMtt102	0.849	0.873	0.805	0.800	0.854	0.797	0.871	0.901	0.909	0.908	0.881	0.882	0.783	0.762	0.809	0.808	0.869	0.934		0.916	0.961	0.937
LMtt103	0.712	0.752	0.678	0.691	0.752	0.669	0.804	0.902	0.830	0.826	0.751	0.791	0.723	0.720	0.727	0.776	0.783	0.845	0.916		0.945	0.880
LMtt104	0.812	0.811	0.680	0.724	0.804	0.743	0.828	0.891	0.849	0.854	0.832	0.806	0.700	0.707	0.754	0.758	0.824	0.902	0.961	0.945		0.943
LMtt105	0.884	0.869	0.688	0.735	0.812	0.805	0.807	0.829	0.838	0.855	0.864	0.822	0.728	0.764	0.802	0.761	0.851	0.923	0.937	0.880	0.943	

The highest level ( $r=0.966$ ) of the similarity measure (Pearson  $r$ ) in pairs of annual TTSS (Tab. 1) was close to the respective estimates found for other lakes (Kamenir *et al.* 2006, 2008). Concomitantly, its minimal level ( $r=0.669$ ), describing a pair of the years (1989 and 2003) at the beginning and the end of the studied process, was found previously only for pairs taken from two different ecosystems (meso-eutrophic Lake Kinneret and oligotrophic Lake Tahoe; Kamenir *et al.* 2008). Both these years look abnormal in their year-groups (Fig. 3 B and E, respective) and represent very different estimates of fraction V2.7. Formally, considering Pearson  $r > 0.9$  as 'high' similarity levels, we can distinguish several 'homogenous periods' – several pairs of years (1984-1985 and 1988-1989; 1990-1991) and following that, three long time-intervals (1992-1995, 1996-2000, and 2002-2004) (Tab. 1). Some years exhibit 'intermediate' TTSS shapes, having high similarity with their neighbors both on the left and right, e.g., the years 1987 and 2001 (Tab. 1). We can see also a high similarity between spectra divided by 5-8 years, e.g., between the years 2000-2001 and 1992-1995 (Tab. 1; Fig. 2). Therefore, we can distinguish a very long 'transitory' time-interval of 1990-2001 (Fig. 2), clearly distinguishable from its predecessor and follower, which have higher similarities between them.

Consequently, we can see the transformation process, divided into several stages (Figs 2 and 3F). This process ended in 2005 with a 'return' to the initial shape (1984), but with a much upgraded height, i.e., the total biodiversity (Fig. 3F). This trend of species number increase is clearly seen in the long-term dynamics curve (Fig. 4A). While the number of large species ( $\text{Log}V > 4$ ) was almost the same – and very low – in 2005, as 20 years earlier, many smaller species were added (Fig.

3F). Therefore, the observed patterns of TTSS evolution are connected with an overall decrease in phytoplankton average cell volume. This reduction exhibited a very clear pattern during the years 1986-1997 (Fig. 4B). Two main trends caused this volume decrease: the size changes occurring inside each algal group and the overall reduction of the assemblage mean size due to the addition of numerous medium-and-small species. Species number change in the most important size fractions had obviously non-linear dynamics: several fractions seem to be linked as a coherent group, while others had an almost opposite phase (Fig. 5A). The 'extreme peripheral' fractions of  $\text{Log}V = -0.3$  and  $0.0$  are the notable exceptions, increasing only during the last years (2000-2005), when the most significant (i.e., including the largest species number) fractions ( $\text{Log}V = 1.8$  and  $2.4$ ) decline (Fig. 5A). The largest cell volume fraction ( $V_{5.1}$  here) is unvarying, as it includes only two species (*Ceratium hirundinella* and *Peridinium willei*) registered each year. The central region ( $V_{1.2}$ - $V_{3.6}$ , excluding  $V_{2.7}$ ) fractions exhibit the most rapid growth and a strong correlation with the total diversity growth ( $r > 0.67$ ,  $p < 0.001$ ,  $n = 22$  for each fraction). Some fractions demonstrate strong and statistically significant paired correlations ( $r > 0.7$ ,  $p < 0.001$ ,  $n = 22$ ), even if they are not 'neighbors'. Two large cell fractions ( $V_{4.5}$  and  $V_{5.1}$ ) show a strong negative correlation ( $r < -0.6$ ) with the total diversity.

While the dynamics of separate fractions was very complicated (Fig. 5A), the total species number grew almost linearly, reaching a new 'asymptote' of 91 species in 2003 (Fig. 4A). While some 'jumps' and drops are notable occasionally, the inter-annual trend is clearly seen (Fig. 4A). The linear regression interpolates this dependence of the total species number vs the time as  $y = 2.51x - 4940.50$ , where  $x$  is the year,  $r^2 = 0.900$ ,  $n = 22$ ,  $p < 0.001$ .

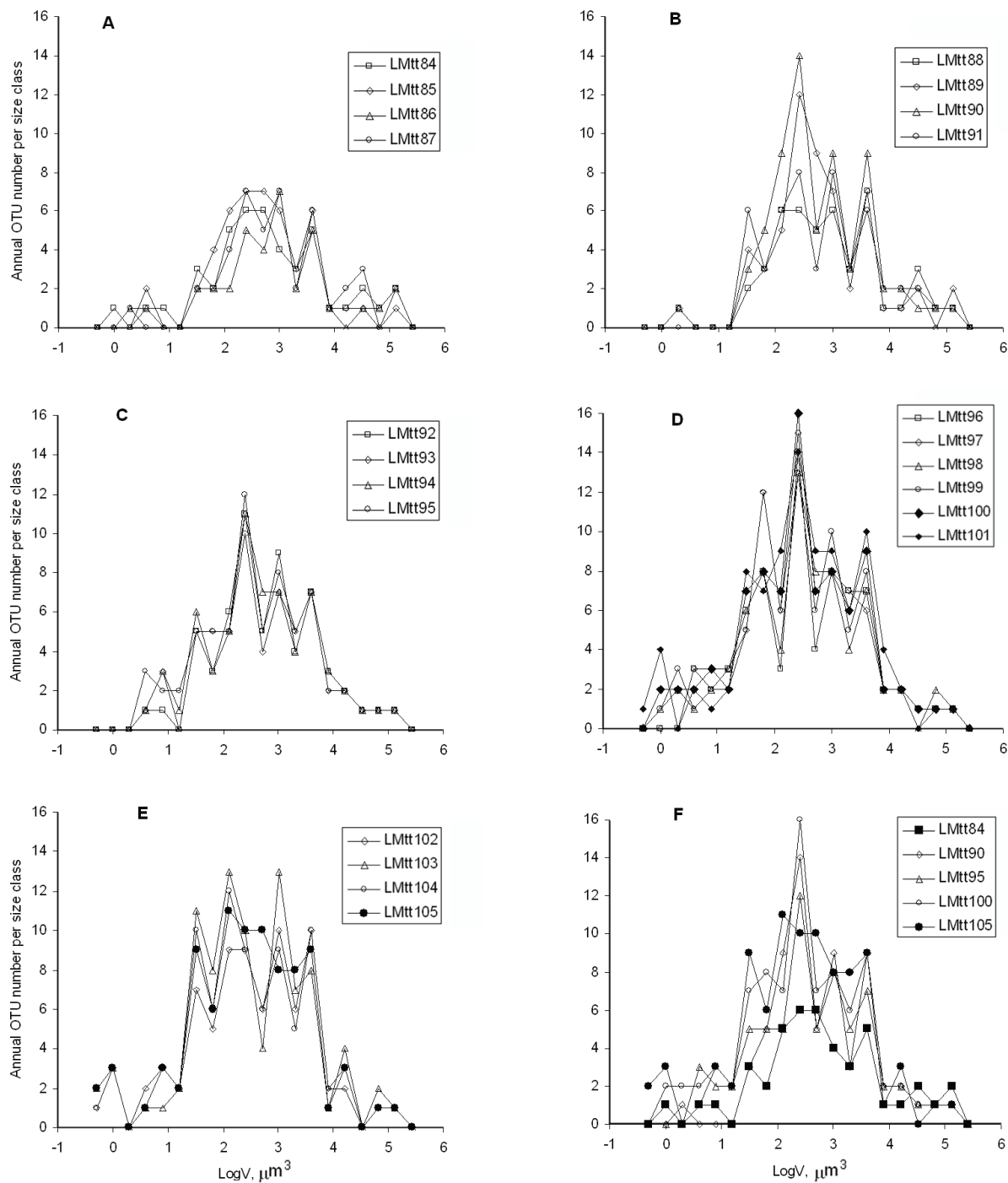


**Fig. 3.** Several periods of L. Maggiore phytoplankton taxonomic size structure change. The consecutive periods (A-E, respectively) are separated with the help of hierarchical cluster analysis (Fig. 2; Tab. 1). The total process of the TTSS evolution (1984-2005) is summarized by a comparison of the consecutive periods (F).

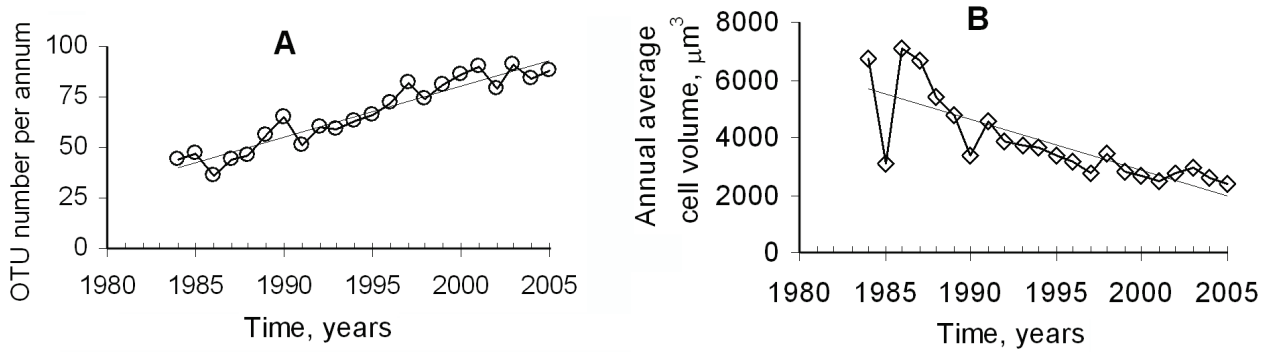


**Fig. 4.** Long-term dynamics (1984-2005) of the annually registered species number (A) and of the annual average cell volume ( $V$ ,  $\mu\text{m}^3$ ) produced by the annual taxon list (B).

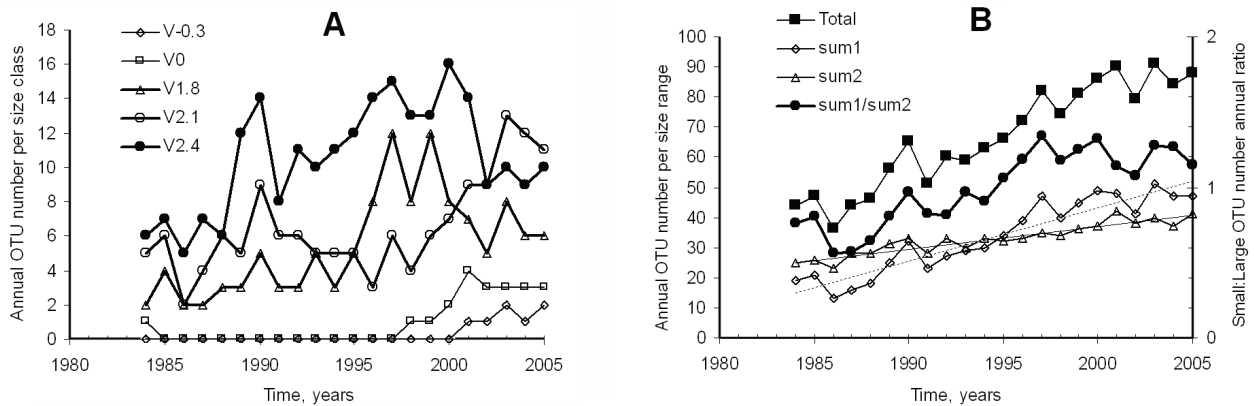


**Fig. 5.** Dynamics of specific size fractions (Figs 1 and 3) of size spectrum (A), and of phytoplankton assemblage total taxonomic diversity (Total) and of two halves ( $\text{Log}V \leq 2.4$  and  $\text{Log}V > 2.4$ , marked as sum1 and sum2, respectively) (B). The ratio of the species number in those two halves ( $\text{sum1}/\text{sum2}^{-1}$ ) is shown using the right Y-axes.

The phytoplankton assemblage seems to be changing as a whole, being more stable and orderly than its separate parts (Fig. 5). Two very different shapes of the phytoplankton taxonomic size structure can be distinguished, characterizing the transitory period and the 'less dynamic years' preceding and following it (Fig. 6A and B). The high similarity of the first and last periods is especially evident after a scale transformation (Fig. 6B). It clearly demonstrates the phytoplankton structural stability supplemented with the diminishing role of the largest species ( $\text{Log}V > 4$ ) during the lake oligotrophication. A significant difference ( $p < 0.001$ ,  $df = 3, 14$ ,  $F = 16.18$ ) was found for size fraction V2.4 (ANOVA one-way with Bonferroni post-tests) between several year-groups selected according to cluster analysis results (Tab. 1). The difference was significant ( $p = 0.021$ ) between groups 1 (years 1984-1989) and 2 (1992-1995), ( $p < 0.01$ ) between groups 1 and 3 (1996-2000), and groups 3 and 4 (2002-2004). The differences between groups 2 and 3, 2 and 4, and 1 and 4 were not significant ( $p > 0.05$ ). Therefore, group 3 seems to be the most illustrative representation of the transition-period type, distinguishable from the two stability periods (1 and 4). Such TTSS properties can be valuable for the

development of the diagnostic classification and quantitative comparison means needed to distinguish between stable and transitional stages.

#### 4. DISCUSSION

Long-term analysis of taxonomic size structure evolution during an apparent lake oligotrophication process (Ruggiu *et al.* 1998) shows many interesting characteristics of integral phytoplankton assemblage adaptation. We can see the transformation process of the lake phytoplankton taxonomic structure – abrupt for some size fractions and almost linear for the total species number (Fig. 5) – coming to a new, more stable situation which reproduced itself during the last 4 years of the study. This transformation is clearly seen when comparing the partial periods (Fig. 3F). After the starting period of 1984-1987, we see almost the same TTSS shapes in 1990-2001 (with notable changes of the central peak at  $\text{Log}V = 2.4$ ), and then a 'return' to the starting shape (1984) during the final period. This return is better appreciated with the help of a scale-transformed comparison between the 'start-and-finish' shapes (Fig. 6B). We see here the same three peaks of almost the same height within the central region, after the pro-

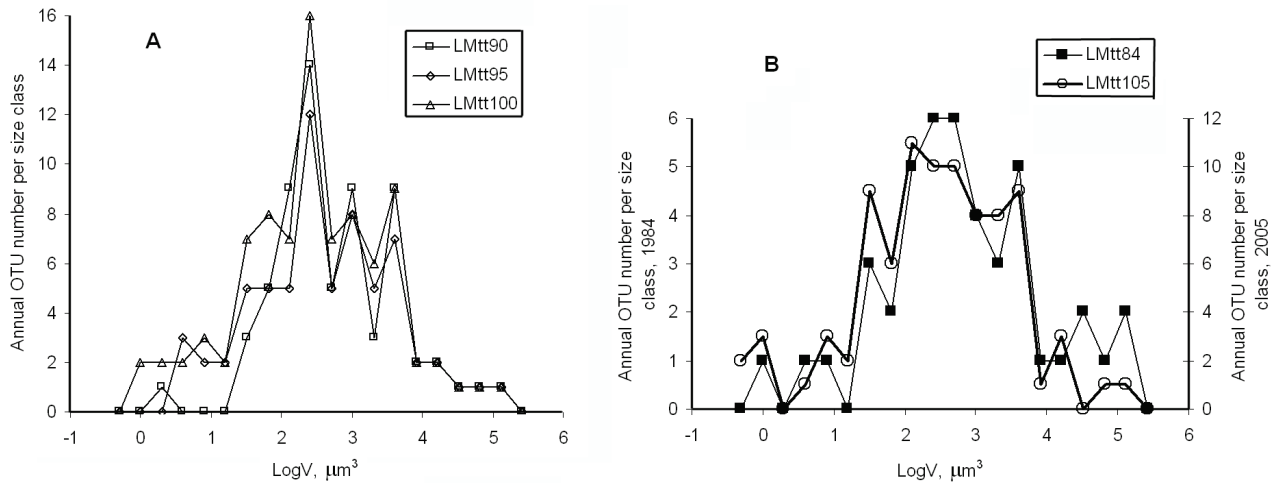


**Fig. 6.** A comparison of the L. Maggiore phytoplankton TTSS-shape (Figs 1 and 3) for several years representing the period of the most noticeable phytoplankton structure transformation – 1990-2001 (A) and for the years preceding (1984-1989) and following it (2002-2005) compared *via* a scale transformation of Y-axes (B).

nounced upgrading and decline of the  $\text{LogV}=2.4$  peak. In reality, the two shapes are similar only while rescaled, as they have a 2 times different height. The 2005 spectrum also has a leftward side-shift, as its small-size region is raised, while the largest species zone ( $\text{LogV}>4$ ) is diminished. This addition of small species ( $\text{LogV}<2$ ) is also evident during the transition period (Fig. 6A). All in all, the species number has grown  $>2$  times, from 44 in 1984 to 90 and more during the last years, mostly due to the addition of small ( $V<100\ \mu\text{m}^3$ ) species (Figs 5-6). The second or transitional period (Fig. 3B-D) is characterized by a gradual growth of the central peak ( $V2.4$ )  $>3$  times, from 5 in 1986 to 11 in 1994, 15 in 1997, and 16 in 2000. Then the central peak (having shown the most drastic dynamics) diminished again to the level of another central peak ( $V3.0$ ; 10 in 2002) and moved left (from  $\text{LogV}=2.4$  to 2.1; Fig. 3E).

The dynamics comparison of numerous size fractions shows a rather complicated process, with rather abrupt increases and declines (Fig. 5A). It is not synchronous for all fractions. While some of them decline drastically, others increase. Some of such cases can be explained by changing grazing pressure (Morabito, unpubl.), and others by the pronounced  $V_j$  changes of some species, resulting in their shift to another size fraction. The total taxonomical diversity growth parallels the average nutrient level decline, though not all size fractions equally profit from these changes. Really, some irregularities and trend-reversals are evident (Fig. 4) which can be explained by the physical environment analysis. Such analysis unveils a rather complicated set of relations. Their detailed description is currently in preparation. The most drastic restructuring is evident within the central region, especially for the notorious fraction V2.4. The most prominent overall changes describe total taxonomic diversity growth, made up mainly by small-cell species (Fig. 5B), and the general

decline (2-3 times) in the average species size (Fig. 4B). Another prominent property, seen with the help of TTSS, is the existence of three clearly different stages, where the first and last have almost the same general pattern of three equal height peaks, while the intermediate transitional stage shows an explicit domination of one central peak (Fig. 3). While each fraction oscillates along time, these oscillations are not strictly coherent. Therefore, the TTSS proportions are changing and may be helpful to analyze the overall structural change dynamics (Fig. 5B). A comparison of the most prominent fraction ( $V2.4$ ) with its neighbors ( $V2.1$  and  $V2.7$ ) depicts the years 1991-2000 as a rather unusual period (Fig. 5A). Such a pronounced change of proportions between several size fractions leads to a notable diminishing of overall size-structure self-similarity (Tab. 1). During all periods, we can see peaks at positions ( $\text{LogV}$ ) of 2.4, 3.0 and 3.6. Only in the last period (2002-2005; Fig. 3E) one of the peaks ( $\text{LogV}=2.4$ ) moved one class leftward ( $\text{LogV}=2.1$ ), while  $\text{LogV}=2.4$  went down. This process is clearly seen via size class dynamics (Fig. 5A), where fraction V2.1 rapidly rose after 1998 while its neighbors (V2.4 and V1.8) quickly declined. The average cell volume decline is seen from the two parts of the spectrum dynamics comparison (Fig. 5B). The linear regression slope for the small species (sum1;  $\text{LogV}\leq 2.4$ ) is  $>2$  times higher than the slope for the rest of the species (sum2;  $\text{LogV}>2.4$ ). Consequently, the ratio between the species number of the small and large parts (sum1 sum2<sup>-1</sup>) changed from 0.57 in 1987 to 1.34 in 1997 (Fig. 5B).

Change in size structure is influenced by many phytoplankton groups. For Chlorophytes and Cryptophytes, the mean cell volume remained stable, but for Chrysophytes, a declining trend was evident. It was produced by the volume reduction of many *Mallomonas* species, and the appearance of some small taxa, such as



*Chrysochromulina parva* and *Ochromonas* sp. The Cyanoprocaryota group showed a very clear reduction in average cell volume, driven by the size decrease of *Microcystis aeruginosa* and *Planktothrix rubescens*, together with the increasing importance – in terms of both cell abundance and species number – of small chroococcales (*Apahnothece*, *Aphanocapsa*, *Cyano-dictyon*, and *Synechococcus*). For diatoms, the reduction was less clear because some species reduced their volume (*Asterionella formosa*, *Aulacoseira ambigua*, *Cyclotella comensis*), while others increased it (*Fragilaria crotonensis*, *Aulacoseira islandica* morf. *helvetica*). Volume maxima of the whole diatom assemblage, observed between 1987 and 1991, were due to *Synedra ulna* v. *danica*. However, lower average cell volumes of the diatoms since the early nineties can be explained by the increasing importance of the species number and relative abundance of small centric diatoms. The clear cell volume decrease of dinoflagellates was due to the appearance of small *Gymnodinium* species. The time course of the size decrease followed the general oligotrophication of the lake: the regression between TP concentration at mixing and mean annual LogV is highly significant ( $\text{LogV} = 1.93 + 0.05 \text{ TP}$ ;  $n=22$ ;  $r=0.62$ ;  $p=0.002$ ). It is very plausible that the rearrangement of the phytoplankton assemblage towards the growing number of smaller species was a consequence of the ecosystem changes related to nutrient reduction. This reduction could have given a growing advantage to species with a higher S/V ratio, being more efficient in assimilating nutrients (Chisholm 1982; Seip & Reynolds 1995). The decrease of phytoplankton size at lower nutrient levels has been frequently observed in lakes (see, for example, Masson *et al.* 2000). For instance, the trophic recovery of Lake Lucerne, a deep Swiss subalpine lake, which underwent a trophic evolution comparable – in terms of temporal dynamics as well as TP concentration involved in the process – to that of Lago Maggiore, was accompanied by an increase in the relative biomass of small *r*-strategist phytoplankton (Bürgi & Stadelmann 2002).

The increasing importance of small *r*-strategists during an oligotrophication process has also been observed in Lake Michigan (Lehman 1991). The rearrangement of the trophic web during the P-level decline could explain this pattern. Small algal taxa are expected to be favored under lower nutrient concentration, because their high surface area to volume ratio enables rapid nutrient exchange through the cell surface (Harris 1994). The reduced grazing pressure could also explain the increasing number of small species. The top-down control (due to large herbivorous crustaceans) is known to decline in the deep lakes undergoing oligotrophication (Lehman 1991; Bürgi & Stadelmann 2002; Manca & Ruggiu 1998).

All in all, the Lago Maggiore TTSS pattern resembles the typical pattern described earlier for Lake Kin-

neret, a warm, meso-eutrophic, monomictic, with a surface area of 170 km<sup>2</sup> (Serruya 1978). Several man-induced changes, followed by a long drought period, have ultimately led to drastically changed phytoplankton composition and annual succession patterns since the mid-1990s (Zohary 2004); however, the TTSS general pattern has survived these extremely unusual years (Kamenir *et al.* 2006). While the two lakes are so different, the stability of their phytoplankton taxonomic size structure is characterized by a comparable level of the applied similarity index (Pearson *r* here). A close level of similarity was also demonstrated by oligotrophic Lake Tahoe, USA (Kamenir *et al.* 2008). In all three lakes, we can see 'more-or-less' the same size distribution resembling a bell symmetrical in LogV scale. In fact, its fine structure can be described as several peaks separated by clearly seen troughs. While the peaks take almost the same horizontal positions (LogV) across a time series, their height fluctuates from year to year (Fig. 3). If very close general patterns (a lognormal distribution dissected by deep troughs to 2-4 main peaks) can be observed across long time intervals (>20 years) in very distant regions, one should look for very general mechanisms producing and supporting such distribution patterns (Havlicek & Carpenter 2001; Kamenir *et al.* 2008). Even a short analysis produces a number of such intertwined mechanisms (Kamenir *et al.* 2008). Therefore, specific studies are needed to select one possible factor and produce a pattern difference sufficiently big and consistent to be estimated quantitatively and compared with the change in the impact factors involved. Here we tried to perform such a study, where one factor – very important, common and sometimes suitable to anthropogenic control, specifically, the phosphorus level – was selected and supported by large-scale information collected during many years. The result gives evidence of the very high consistency of the TTSS general shape, accompanied by statistically significant differences in some peak heights, suitable to differentiation between two subsets of this pattern. Detailed comparisons of the peak heights and side shifts allow us to divide the total period of the L. Maggiore study into three stages (taking years 1990-2001 together) characterized with more homogenous TTSS patterns (Figs 2 and 6).

## 5. CONCLUSIONS

The results obtained from this study confirm our working hypotheses: 1) Reliable structural features were found in the TTSS general pattern of the Lago Maggiore phytoplankton, when many principal environmental characteristics changed considerably during the long-term oligotrophication process. 2) At the same time, the fine structure of TTSS reveals features that helped us divide the total oligotrophication process into three stages characterized with notable differences in the central peaks' proportions. These height changes within

the central region were caused by pronounced alterations of the species list and the overall taxonomic diversity of the lake phytoplankton. Typical patterns of the stable and transitory stages were differentiated, which could be valuable for environmental protection and ecological diagnostics. Oligotrophication process decomposition was supported by quantitative statistical estimators. This way, TTSS can be applied as a means of quantitative analysis for integral natural community structural evolution. Such an approach would facilitate application of the phytoplankton assemblage taxonomic structure in development of analytical tools acutely needed by environmental management, monitoring, and theoretical ecology.

#### ACKNOWLEDGEMENTS

We acknowledge the assistance of Pierisa Panzani for calculating cell volumes of Lago Maggiore phytoplankton throughout the whole time series, and Alessandro Oggioni for improving the measuring procedure. The EC INTAS-6196 grant to YK enabled size spectrum analysis. We are grateful to Zvy Dubinsky, John Hall, Antonina Popova, Alexander Prazukin, and Tamar Zohary for valuable discussions and advice. We highly appreciate constructive ideas and helpful comments of two unknown reviewers. We also thank Sharon Victor for providing priceless help in manuscript preparation and language editing.

#### REFERENCES

- Anagnostidis, K. & J. Komárek. 1988. Modern approach to the classification system of Cyanophytes. 3-Oscillatoriales. *Arch. Hydrobiol., Suppl. 80, Algological Studies*, 50-53: 327-472.
- Baldi, E. 1949. La situation actuelle de la recherche limnologique après le Congrès de Zurich. *Revue suisse Hydrol.*, 11: 637-649 (in French).
- Begon, M., J.L. Harper & C.R. Townsend. 1996. *Ecology: Individuals, Populations and Communities*. 3<sup>rd</sup> ed. Blackwell, London: 945 pp.
- Bürgi, H.R. & P. Stadelmann. 2002. Alteration of phytoplankton structure in Lake Lucerne due to trophic conditions. *Aquatic Ecosystem Health and Management*, 5: 45-59.
- Cha, S.-H. & S. N. Srihari. 2002. On measuring the distance between histograms. *Pattern Recognition*, 35: 1355-1370.
- Chisholm, S.W. 1992. Phytoplankton size. In: Falkowski, P. G. & A. D. Woodhead (Eds), *Primary Productivity and Biogeochemical Cycles in the Sea*. Plenum Press, New York, NY: 213-237.
- de Bernardi, R., G. Giussani, M. Manca & D. Ruggiu. 1988. Long-term dynamics of plankton communities in Lago Maggiore (N. Italy). *Verh. int. Ver. Limnol.*, 23: 729-733.
- Guilizzoni, P., G. Bonomi, G. Galanti & D. Ruggiu. 1983. Relationship between sedimentary pigments and primary production: evidence from core analyses of twelve Italian lakes. *Hydrobiologia*, 103: 103-106.
- Havlicek, T. D. & S. R. Carpenter. 2001. Pelagic species size distributions in lakes: are they discontinuous? *Limnol. Oceanogr.*, 46: 1021-1033.
- Harris, G.P. 1994. Patterns, process and prediction in aquatic ecology: a limnological view of some general ecological problems. *Freshwat. Biol.*, 32: 143-160.
- Hemmingsen, A. M., 1934. A statistical analysis of the differences in body size in related species. *Vidensk. Medd. Natur. Foren.*, 98: 125-160.
- Hillebrand, H., C.-D. Dürselen, D. Kirschtel, U. Pollinger & T. Zohary. 1999. Biovolume calculation for pelagic and benthic microalgae. *J. Phycology*, 35: 403-424.
- Hutchinson, G. E. & R. H. MacArthur. 1959. A theoretical ecological model of size distributions among species of animals. *Am. Nat.*, 93: 117-125.
- Kamenir, Y., Z. Dubinsky, & T. Zohary. 2006. The long-term patterns of phytoplankton taxonomic size-structure and their sensitivity to perturbation: A Lake Kinneret case study. *Aquat. Sci.*, 68: 490-501.
- Kamenir Y., M. Winder, Z. Dubinsky, T. Zohary & G. Schladow. 2008. Lake Tahoe vs. Lake Kinneret phytoplankton: comparison of long-term taxonomic size structure consistency. *Aquat. Sci.*, 70: 195-203.
- Lehman, J.T. 1991. Causes and consequences of cladoceran dynamics in Lake Michigan: implications of species invasion by *Bythotrephes*. *J. Great Lakes Res.*, 17: 437-445.
- Lund, J.W.G., C. Kipling & E. D. Le Cren. 1958. The inverted microscope method of estimating algal numbers and the statistical basis of estimations by counting. *Hydrobiologia*, 11: 143-170.
- Manca, M & D. Ruggiu. 1998. Consequences of pelagic food-web changes during a long-term lake oligotrophication process. *Limnol. Oceanogr.*, 43: 1368-1373.
- Manca, M., A. Calderoni & R. Mosello. 1992. Limnological research in Lago Maggiore: studies on hydrochemistry and plankton. *Mem. Ist. ital. Idrobiol.*, 50: 171-200.
- Masson, S., B. Pinel-Alloul & V.H. Smith. 2000. Total phosphorus-chlorophyll-*a* size fraction relationships in southern Quebec lakes. *Limnol. Oceanogr.*, 45: 732-740.
- Morabito, G. & A. Pugnetti. 2000. Primary productivity and related variables in the course of the trophic evolution of Lake Maggiore. *Verh. int. Ver. Limnol.*, 27: 2934-2937.
- Mosello, R. & D. Ruggiu. 1985. Nutrient load, trophic conditions and restoration prospects of Lake Maggiore. *Int. Revue ges. Hydrobiol.*, 70: 63-75.
- Odum, E. P., 1971. *Fundamentals of Ecology*. Saunders, Philadelphia: 574 pp.
- Ravera, O. & R.A. Vollenweider. 1968. *Oscillatoria rubescens* D.C. as an indicator of Lago Maggiore eutrophication. *Schweiz Z. Hydrol.*, 30: 374-380.
- Ruggiu, D., G. Morabito, P. Panzani & A. Pugnetti. 1998. Trends and relations among basic phytoplankton characteristics in the course of the long-term oligotrophication of Lake Maggiore (Italy). *Hydrobiologia*, 369-370: 243-257.
- Salmaso, N., G. Morabito, L. Garibaldi, & R. Mosello. 2007. Trophic development of the deep lakes south of the Alps: a comparative analysis. *Arch. Hydrobiol., Fundamental and Applied Limnology*, 170: 177-196.
- Seip, K. L. & C. S. Reynolds. 1995. Phytoplankton functional attributes along trophic gradient and season. *Limnol. Oceanogr.*, 40: 589-597.
- Serruya, C. (ed.). 1978. *The Kinneret. Monographia Biologica*. Dr W. Junk Publishers, The Hague: 455 pp.
- Sheldon, R.W., A. Prakash & W.H. Sutcliffe. 1972. The size distribution of particles in the ocean. *Limnol. Oceanogr.*, 17: 27-340.
- Smith, F.A., J.H. Brown, J.P. Haskell, S.K. Lyons, J. Alroy, E.L. Charnov, T. Dayan, B.J. Enquist, S.K.M. Ernest, E.A. Hadly, K.E. Jones, D.M. Kaufmann, P.A. Marquet, B.A. Maurer, K.J. Niklas, W.P. Porter, B. Tiffney, M.R. Willig. 2004. Similarity of mammalian body size across the taxonomic hierarchy and across space and time. *Am. Nat.*, 163: 672-691.
- Sneath, P. H. A. & R. R. Sokal. 1973. *Numerical Taxonomy*. Freeman, San Francisco: 576 pp.
- Sprules, W. G. & M. Munawar. 1986. Plankton size spectra in relation to ecosystem productivity, size, and perturbation. *Can. J. Fish. aquat. Sci.*, 43: 1789-1794.

Thibault, K. M., E. P. White & S. K. M Ernest. 2004. Temporal dynamics in the structure and composition of a desert rodent community. *Ecology*, 85: 2649-2655.

Zohary, T. 2004. Changes to the phytoplankton assemblage of Lake Kinneret after decades of a predictable, repetitive pattern. *Freshwat. Biol.*, 49: 1355-1371.

## A P P E N D I X

**Tab. 2.** Operational taxonomic unit (OTU) list of Lago Maggiore phytoplankton. OTUs registered in the lake during twenty two years (1984-2005) are listed according to their typical cell volume estimate ( $V$ ,  $\mu\text{m}^3$ ). Size class is defined by the upper border of cell volume included in it and expressed as  $\log_{10}(V)$  estimate given in parentheses. Taxonomic groups are: CHR – Chrysophyceae, CYA – Cyanoprokaryota, CRY – Cryptophyta, DIA – Diatomea, CHLO – Chlorophyta, and DINO – Dinophyta.

Taxonomic group	Operational Taxonomic Unit (OTU)	Cell Volume ( $V$ , $\mu\text{m}^3$ )	LogV	Size Class: The volume range and the upper border log	
CYA	<i>Aphanothece clathrata</i> (01-02)	0.4	-0.40	<=0.5 (-0.3)	
CYA	<i>Aphanothece smithii</i> (03-05)	0.4	-0.40		
CYA	<i>Aphanothece</i> sp.1	0.4	-0.40		
CYA	Cfr. <i>Cyanobium</i> sp.	0.5	-0.30		
CYA	<i>Aphanocapsa incerta</i>	0.6	-0.22		>0.5-1 (0.0)
CYA	<i>Aphanothece bachmannii</i>	0.6	-0.22		
CYA	<i>Aphanothece</i> cf. <i>floccosa</i> (01-02)	0.6	-0.22		
CYA	<i>Aphanothece smithii</i> (02)	0.6	-0.22		
CYA	<i>Aphanothece</i> sp.2	0.6	-0.22		
CYA	Cfr. <i>Aphanocapsa delicatissima</i> (99-05)	0.7	-0.15		
CYA	<i>Aphanothece</i> cf. <i>floccosa</i> (03-05)	0.8	-0.10		
CYA	<i>Aphanothece smithii</i> (01)	0.8	-0.10		
CYA	Cfr. <i>Aphanocapsa delicatissima</i> (98)	0.8	-0.10		
CYA	<i>Microcystis incerta</i>	1.0	0.00	>1-2 (0.3)	
CYA	<i>Aphanothece clathrata</i> (98-00)	1.1	0.04		
CYA	<i>Aphanothece smithii</i> (99-00)	1.1	0.04		
CHLO	<i>Hyaloraphidium contortum</i>	1.2	0.08		
CYA	<i>Aphanothece clathrata</i> (86-90)	1.3	0.11		>2-4 (0.6)
CHLO	<i>Lyngbya limnetica</i>	2.7	0.43		
CYA	<i>Aphanothece clathrata</i> (92-97)	3.3	0.52		
CYA	<i>Aphanothece smithii</i> (95-97)	3.3	0.52		
CHLO	<i>Choricystis coccoides</i>	3.3	0.52		
CYA	<i>Cyanodictyon planctonicum</i>	3.3	0.52		
CHLO	<i>Lobocystis</i> sp.(05)	4.1	0.61	>4-8 (0.9)	
CYA	<i>Synechococcus</i> sp.	4.1	0.61		
CYA	<i>Aphanothece</i> cf. <i>floccosa</i> (95-00)	4.2	0.62		
CYA	<i>Aphanocapsa</i> cfr. <i>elachista</i>	4.6	0.66		
DINO	<i>Peridinium</i> sp.	5.0	0.70		
CHLO	<i>Lobocystis</i> sp. (84-04)	5.3	0.72		
CHLO	<i>Dictyosphaerium</i> sp.	6.2	0.79		
CYA	<i>Microcystis aeruginosa</i> (92-94)	6.4	0.81		
CHLO	<i>Gloecapsa</i> sp.	6.8	0.83		
CYA	<i>Pseudoanabaena</i> sp. (04-05)	7.1	0.85		>8-16 (1.2)
CYA	<i>Lyngbya</i> sp.	7.8	0.89		
CHR	Cfr. <i>Ochromonas</i> sp.	9.3	0.97		
CHLO	<i>Stichococcus minutissimus</i>	9.8	0.99		
CYA	<i>Leptolyngbya</i> sp.	10.3	1.01	>16-32 (1.5)	
CYA	<i>Oscillatoria limnetica</i>	17.0	1.23		
CYA	<i>Pseudanabaena limnetica</i> (91)	17.0	1.23		
CHLO	<i>Tetrachlorella incerta</i>	17.4	1.24		
CHLO	<i>Monoraphidium circinale</i>	18.6	1.27		
CYA	<i>Limnothrix</i> sp. (92-93)	19.0	1.28		
CYA	<i>Pseudoanabaena</i> sp. (91)	19.0	1.28		
CYA	<i>Snowella lacustris</i> (84-91)	20.0	1.30		
CYA	<i>Limnothrix</i> sp. (94-05)	21.0	1.32		
CYA	<i>Pseudanabaena acicularis</i>	21.0	1.32		
CYA	<i>Pseudanabaena</i> sp. (84)	21.0	1.32	(continued)	
CYA	<i>Pseudanabaena catenata</i>	21.5	1.33		
DIA	<i>Cyclotella pseudostelligera</i> (92-98)	22.0	1.34		
DIA	<i>Cyclotella stelligeroides</i>	22.0	1.34		
DIA	<i>Thalassiosira pseudonana</i>	22.0	1.34		

(continued)

Tab. 2. Continuation (page 2).

Taxonomic group	Operational Taxonomic Unit (OTU)	Cell Volume (V, $\mu\text{m}^3$ )	LogV	Size Class: The volume range and the upper border log
CYA	<i>Pseudoanabaena</i> sp. (89-90)	23.0	1.36	
CYA	<i>Microcystis aeruginosa</i> (91)	24.0	1.38	
CHLO	<i>Scourfieldia cordiformis</i>	24.0	1.38	
CHLO	<i>Crucigeniella rectangularis</i>	24.5	1.39	
CYA	<i>Pseudoanabaena</i> sp. (93)	24.5	1.39	
CHLO	<i>Coelastrum</i> sp.	25.3	1.40	
CHLO	<i>Ankyra judayi</i>	25.5	1.41	
CYA	<i>Snowella lacustris</i> (92-05)	26.0	1.41	
CHLO	<i>Sphaeroeca volvox</i>	26.8	1.43	
DIA	<i>Cyclotella pseudostelligera</i> (00-01)	28.0	1.45	
DIA	<i>Stephanocostis chantaicus</i>	28.0	1.45	
CYA	<i>Pseudanabaena limnetica</i> (01-05)	29.8	1.47	
CHR	<i>Chrysidalis</i> sp.	31.0	1.49	
DIA	<i>Cyclotella pseudostelligera</i> (02-05)	31.0	1.49	
CYA	<i>Geitherinema acuiforme</i>	31.0	1.49	
CYA	<i>Pseudoanabaena</i> sp. (94)	31.4	1.50	
DIA	<i>Cyclotella comensis</i> mor. <i>minima</i> (05)	35.0	1.54	>32-64 (1.8)
CHLO	<i>Scenedesmus obtusus</i> f. <i>alternans</i>	37.0	1.57	
CHLO	<i>Scenedesmus linearis</i>	38.0	1.58	
DIA	<i>Cyclotella comensis/gordonensis</i> (00-01)	40.0	1.60	
CYA	<i>Pseudanabaena limnetica</i> (99-00)	40.7	1.61	
CHLO	<i>Lagerheimia subsalsa</i>	41.7	1.62	
CYA	<i>Oscillatoria</i> sp. (85)	43.0	1.63	
CHLO	<i>Dictyosphaerium pulchellum</i> (01)	44.0	1.64	
CHLO	<i>Ankyra lanceolata</i>	44.9	1.65	
DIA	<i>Cyclotella pseudostelligera</i> (91)	45.0	1.65	
CYA	Cfr. <i>Oscillatoria</i>	47.0	1.67	
DIA	<i>Cyclotella comensis/gordonensis</i> (99)	48.0	1.68	
DIA	<i>Cyclotella</i> sp. (1)	48.0	1.68	
CYA	<i>Planktothrix rubescens</i> (99)	50.0	1.70	
CHR	<i>Chrysochromulina parva</i>	50.7	1.71	
CYA	<i>Pseudanabaena limnetica</i> (95-98)	51.2	1.71	
CYA	<i>Aphanizomenon issatschenkoi</i>	53.0	1.72	
CHLO	<i>Monoraphidium komarkovae</i>	53.0	1.72	
CYA	<i>Anabaena flos-aquae</i>	55.0	1.74	
CHLO	<i>Chlamydomonas</i> sp. (1)	55.0	1.74	
CHLO	<i>Monoraphidium minutum</i>	55.0	1.74	
CHLO	<i>Gloeotila pelagica</i>	56.0	1.75	
DIA	<i>Cyclotella pseudostelligera</i> (99)	57.0	1.76	
DIA	<i>Stephanocostis chantaicus</i> (99, 01)	57.0	1.76	
CYA	<i>Planktothrix rubescens</i> (00-05)	58.0	1.76	
CHLO	<i>Ankistrodesmus</i> sp.	59.0	1.77	
CYA	<i>Microcystis aeruginosa</i> (84-90)	59.0	1.77	
DIA	<i>Cyclotella</i> sp. (3)	60.0	1.78	
CHR	<i>Pseudokephyron</i> sp.	60.0	1.78	
CHR	<i>Uroglena americana</i>	60.0	1.78	
CHLO	<i>Monoraphidium contortum</i> (96-99)	62.0	1.79	
CYA	<i>Aphanizomenon flos-aquae</i> (96-98)	62.6	1.80	
CYA	<i>Planktothrix rubescens</i> (96-98)	63.0	1.80	
DIA	<i>Stephanodiscus parvus</i> (88-91)	64.0	1.81	
CYA	<i>Oscillatoria</i> sp. (84)	69.0	1.84	>64-128 (2.1)
CYA	<i>Planktothrix rubescens</i> (84-93, 95)	69.0	1.84	
CHLO	<i>Scenedesmus bijugatus</i>	71.0	1.85	
CYA	<i>Aphanizomenon flos-aquae</i> (90-95)	74.1	1.87	
CYA	<i>Oscillatoria</i> sp. (87-88)	75.0	1.88	
CYA	<i>Planktothrix rubescens</i> (94)	75.0	1.88	
DIA	<i>Cyclostephanos dubius</i>	77.0	1.89	
CHR	<i>Uroglena</i> sp.	79.0	1.90	
CHR	<i>Dinobryon petiolatum</i>	80.0	1.90	
CHLO	<i>Botryococcus braunii</i>	85.0	1.93	
CYA	<i>Tychonema sequanum</i> (04)	85.0	1.93	
CRY	<i>Plagioselmis nannoplanctica</i> (99-05)	91.0	1.96	
CHLO	<i>Coelastrum sphaericum</i>	92.0	1.96	

(continued)



Tab. 2. Continuation (page 3).

Taxonomic group	Operational Taxonomic Unit (OTU)	Cell Volume (V, $\mu\text{m}^3$ )	LogV	Size Class: The volume range and the upper border log
CHLO	<i>Schroederia setigera</i>	92.0	1.96	
DIA	<i>Cyclotella comensis</i> mor. <i>minima</i> (04)	92.4	1.97	
CYA	Cfr. <i>Phormidium</i> sp.	93.0	1.97	
CYA	<i>Oscillatoria</i> cfr. <i>tenuis</i>	93.0	1.97	
CHLO	<i>Monoraphidium contortum</i> (84-85)	95.0	1.98	
CYA	<i>Aphanizomenon flos-aquae</i> (99-05)	97.0	1.99	
DIA	<i>Cyclotella comensis</i> (03-04)	97.0	1.99	
DIA	<i>Cyclotella comensis</i> mor. <i>minima</i> (03)	97.5	1.99	
DIA	<i>Cyclotella comensis</i> (05)	99.6	2.00	
CHLO	<i>Ankyra</i> sp.	100.0	2.00	
DIA	<i>Synedra acus</i> var. <i>radians</i> small	100.0	2.00	
DIA	<i>Cyclotella comensis</i> mor. <i>minima</i> (02)	100.6	2.00	
DIA	<i>Cyclotella comensis</i> (01-02)	101.0	2.00	
CYA	<i>Tychonema sequanum</i> (05)	101.0	2.00	
CHLO	<i>Nephrocystium lunatum</i>	104.0	2.02	
DIA	<i>Stephanodiscus parvus</i> (92-05)	105.0	2.02	
CHLO	<i>Gonium pectorale</i>	111.0	2.05	
DIA	<i>Cyclotella comensis</i> mor. <i>minima</i> (99-01)	117.0	2.07	
CHR	<i>Dinobryon sociale</i> (03-05)	121.0	2.08	
CHR	<i>Dynobryon cylindricum</i>	121.0	2.08	
CHLO	<i>Dictyosphaerium pulchellum</i>	123.0	2.09	
CRY	<i>Rhodomonas lacustris</i> (00-05)	124.0	2.09	
CHR	Cfr. <i>Chrysamoeba</i> sp.	134.0	2.13	>128-256 (2.4)
CHLO	<i>Sphaerocystis schroeteri</i> (03)	138.0	2.14	
CRY	<i>Plagioselmis nannoplantica</i> (84-99)	139.0	2.14	
DIA	<i>Cyclotella comensis</i> (84-91)	140.0	2.15	
DIA	<i>Cyclotella</i> sp. (2)	140.0	2.15	
DIA	<i>Nitzschia actinastroides</i>	140.0	2.15	
CHLO	<i>Coelastrum astroideum</i>	141.0	2.15	
CRY	<i>Rhodomonas lens</i> (00-01)	157.0	2.20	
CHLO	<i>Scenedesmus quadricauda</i>	159.0	2.20	
DIA	<i>Stephanodiscus minutulus</i> (02-03)	159.0	2.20	
CHLO	<i>Micractinium quadrisetum</i>	160.0	2.20	
CHLO	<i>Sphaerocystis schroeteri</i> (91-02, 04-05)	162.0	2.21	
CYA	<i>Chroococcus limneticus</i>	171.0	2.23	
DIA	<i>Cyclotella comensis</i> (00)	174.0	2.24	
CHR	<i>Dinobryon sociale</i> (00-01)	174.0	2.24	
CYA	<i>Anabaena spiroides</i> (92)	177.0	2.25	
CHLO	<i>Monoraphidium griffithii</i>	179.0	2.25	
CHLO	<i>Gemelliscystis neglecta</i>	180.0	2.26	
CHLO	<i>Pediastrum boryanum</i>	180.0	2.26	
CHLO	<i>Pseudosphaerocystis neglecta</i> (97-01)	180.0	2.26	
CRY	<i>Rhodomonas</i> sp.	180.0	2.26	
CHLO	<i>Paulschulzia pseudovolvox</i> (01-04)	185.0	2.27	
CHR	<i>Mallomonas akrokomos</i>	187.0	2.27	
CHLO	<i>Scenedesmus obtusus</i> f. <i>obtusus</i>	187.0	2.27	
CHLO	<i>Pandorina morum</i>	188.0	2.27	
CHLO	<i>Elakatothrix gelatinosa</i>	190.0	2.28	
CYA	<i>Anabaena lemmermannii</i> (05)	192.0	2.28	
CRY	Cfr. <i>Chroomonas</i> sp. (96-01)	195.0	2.29	
CRY	<i>Katablepharis ovalis</i>	195.0	2.29	
CHR	<i>Dinobryon sociale</i> (94, 97-99)	200.0	2.30	
DIA	<i>Fragilaria capucina</i> (small)	200.0	2.30	
CHLO	<i>Scenedesmus armatus</i>	200.0	2.30	
CRY	<i>Rhodomonas lacustris</i> (84-99)	203.0	2.31	
DIA	<i>Cyclotella comensis</i> (95-96)	204.0	2.31	
DIA	<i>Achnanthes minutissima</i>	205.0	2.31	
CHLO	<i>Kirchneriella obesa</i> v. <i>major</i>	208.0	2.32	
DIA	<i>Stephanodiscus hantzschii</i> (04)	211.0	2.32	
CHLO	<i>Chlamydomonas</i> sp.	212.0	2.33	
CHLO	<i>Paulschulzia pseudovolvox</i> (05)	212.0	2.33	
CYA	<i>Chroococcus limneticus</i> var. <i>elegans</i>	213.0	2.33	
DIA	<i>Cyclotella comensis</i> (92-93)	214.0	2.33	
CHR	<i>Dinobryon bavaricum</i>	215.0	2.33	

(continued)

Tab. 2. Continuation (page 4).

Taxonomic group	Operational Taxonomic Unit (OTU)	Cell Volume (V, $\mu\text{m}^3$ )	LogV	Size Class: The volume range and the upper border log
CYA	<i>Anabaena</i> sp.	217.0	2.34	
CHLO	<i>Coelastrum microporum</i>	218.0	2.34	
CHLO	<i>Coelastrum polychordum</i>	220.0	2.34	
CHLO	<i>Coelastrum reticulatum</i> (03, 05)	220.0	2.34	
CHLO	<i>Coelastrum reticulatum</i> (84-01)	229.0	2.36	
CRY	Cfr. <i>Chroomonas</i> sp. (95)	230.0	2.36	
DIA	<i>Cyclotella</i> cfr. <i>hakanssoniae</i>	236.0	2.37	
DIA	<i>Cyclotella comensis</i> (94)	238.0	2.38	
CHLO	<i>Elakatothrix viridis</i>	240.0	2.38	
CYA	<i>Anabaena</i> cfr. <i>affinis</i>	242.0	2.38	
CHLO	<i>Coelastrum reticulatum</i> v. <i>cubanum</i> (95-98)	245.0	2.39	
DIA	<i>Achnanthes minutissima</i> var. <i>cryptocephala</i>	250.0	2.40	
CHLO	<i>Monoraphidium contortum</i> (88-95)	250.0	2.40	
CHLO	<i>Sphaerocystis schroeteri</i> (84-90)	257.0	2.41	>256-512 (2.7)
CHLO	<i>Tetraedron minimum</i>	260.0	2.41	
CHLO	<i>Nephrocystium limneticum</i>	265.0	2.42	
CHLO	<i>Coelastrum morum</i>	268.0	2.43	
CHLO	<i>Nephrocystium</i> sp.	273.0	2.44	
CHR	<i>Dinobryon divergens</i> var. <i>schauinslandii</i>	289.0	2.46	
DIA	<i>Cyclotella comensis</i> (99)	289.1	2.46	
CRY	<i>Rhodomonas lens</i> (05)	302.0	2.48	
DIA	<i>Cyclotella comensis</i> (97-98)	304.0	2.48	
CHLO	<i>Eudorina unicocca</i>	305.0	2.48	
DIA	<i>Stephanodiscus minutulus</i> (01, 04-05)	307.0	2.49	
CHR	<i>Dinobryon sertularia</i>	317.0	2.50	
CHLO	<i>Lagerheimia citriformis</i>	324.0	2.51	
CHLO	<i>Bitrichia chodati</i>	328.0	2.52	
CHLO	<i>Oocystis lacustris</i>	331.0	2.52	
CHLO	<i>Eudorina elegans</i>	344.0	2.54	
CHLO	<i>Gloeocystis planctonica</i>	350.0	2.54	
DIA	<i>Cyclotella cyclopuncta</i> (small)	391.0	2.59	
CHR	<i>Dinobryon divergens</i> (94-05)	397.0	2.60	
DIA	<i>Cyclotella</i> cfr. <i>praetermissa</i> (98)	402.0	2.60	
DIA	<i>Asterionella formosa</i> (05)	412.0	2.61	
DIA	<i>Cyclotella</i> sp. (4)	430.0	2.63	
DIA	<i>Cyclotella glabriuscula</i>	436.0	2.64	
DIA	<i>Fragilaria crotonensis</i> (84-01)	440.0	2.64	
CHLO	<i>Closterium acutum</i> v. <i>variabile</i> (05)	459.0	2.66	
DIA	<i>Cyclotella distinguenda</i>	477.0	2.68	
DIA	<i>Fragilaria capucina</i> (large)	497.0	2.70	
CHLO	<i>Micractinium pusillum</i>	500.0	2.70	
CHLO	<i>Pediastrum duplex</i>	500.0	2.70	
CHLO	<i>Closterium acutum</i> v. <i>variabile</i> (84-02, 04)	505.0	2.70	
DIA	<i>Fragilaria crotonensis</i> (05)	537.0	2.73	>512-1024 (3.0)
DINO	<i>Gymnodinium</i> sp. (5)	539.0	2.73	
CHR	<i>Mallomonas tonsurata</i> v. <i>alpina</i>	552.0	2.74	
DIA	<i>Cyclotella cyclopuncta</i> (large)	619.0	2.79	
CHR	<i>Mallomonas crassisquama</i>	637.0	2.80	
DIA	<i>Aulacoseira granulata</i>	650.0	2.81	
DIA	<i>Cyclotella ocellata</i> (small)	650.0	2.81	
CHLO	<i>Mougeotia</i> sp. (97)	651.7	2.81	
DIA	<i>Asterionella formosa</i> (02-04)	667.0	2.82	
CHLO	<i>Closterium acutum</i> v. <i>variabile</i> (03)	670.0	2.83	
DINO	<i>Gymnodinium lacustre</i>	690.0	2.84	
DIA	<i>Aulacoseira ambigua</i> (99-05)	693.0	2.84	
CRY	<i>Cryptomonas erosa</i> v. <i>reflexa</i> (86/90-05)	700.0	2.85	
DIA	<i>Diatoma tenuis</i> (02-05)	709.0	2.85	
DIA	<i>Synedra acus</i> v. <i>angustissima</i> (84-86)	773.0	2.89	
CHR	<i>Dinobryon divergens</i> (86-93)	800.0	2.90	
CHR	<i>Dinobryon sociale</i> (87-90)	800.0	2.90	
CHLO	<i>Mougeotia</i> sp. (05)	809.4	2.91	
DIA	<i>Fragilaria crotonensis</i> (02-04)	819.0	2.91	
CHLO	<i>Mougeotia</i> sp. (02-04)	843.2	2.93	

(continued)

Tab. 2. Continuation (page 5).

Taxonomic group	Operational Taxonomic Unit (OTU)	Cell Volume (V, $\mu\text{m}^3$ )	LogV	Size Class: The volume range and the upper border log
DIA	<i>Rhizosolenia eriensis</i> f. <i>brevispina</i>	870.0	2.94	
DIA	<i>Rhizosolenia eriensis</i> v. <i>morsa</i>	870.0	2.94	
DIA	<i>Synedra acus</i> v. <i>angustissima</i> (87-05)	873.0	2.94	
CHLO	<i>Mougeotia</i> sp. (84-96, 98-01)	877.0	2.94	
DIA	<i>Cymbella ventricosa</i>	890.0	2.95	
DIA	<i>Asterionella formosa</i> (84-01)	984.0	2.99	
DIA	<i>Diatoma tenue</i> (85-01)	1000.0	3.00	
DIA	<i>Stephanodiscus</i> sp. (1)	1000.0	3.00	
DIA	<i>Stephanodiscus</i> sp. (2)	1087.0	3.04	>1024-2048 (3.3)
CYA	<i>Platymonas cordiformis</i>	1108.0	3.04	
DIA	<i>Aulacoseira ambigua</i> (92-97)	1237.0	3.09	
DIA	<i>Aulacoseira islandica</i> morf. <i>helvetica</i> (84-91, 94-95)	1237.0	3.09	
DIA	<i>Cyclotella radios</i>	1258.0	3.10	
DIA	<i>Aulacoseira islandica</i> morf. <i>helvetica</i> (93,01,05)	1324.8	3.12	
DIA	<i>Cyclotella ocellata</i> (large)	1374.0	3.14	
CRY	Cfr. <i>Cryptomonas</i> sp. (96)	1386.0	3.14	
DIA	<i>Aulacoseira islandica</i> morf. <i>helvetica</i> (00)	1412.6	3.15	
DIA	<i>Synedra acus</i> var. <i>radians</i> large	1414.0	3.15	
DIA	<i>Aulacoseira islandica</i> morf. <i>helvetica</i> (03)	1421.8	3.15	
CHLO	<i>Carteria</i> sp. (96-03, 05)	1454.0	3.16	
DIA	<i>Aulacoseira islandica</i> morf. <i>helvetica</i> (96)	1571.5	3.20	
DIA	<i>Cyclotella</i> cfr. <i>praetermissa</i> (97)	1578.0	3.20	
DIA	<i>Aulacoseira islandica</i> morf. <i>helvetica</i> (04)	1588.2	3.20	
DINO	<i>Peridinium inconspicuum</i> (03)	1621.0	3.21	
DIA	<i>Aulacoseira islandica</i> morf. <i>helvetica</i> (92)	1636.1	3.21	
DIA	<i>Aulacoseira islandica</i> morf. <i>helvetica</i> (97)	1655.1	3.22	
CRY	<i>Cryptomonas ovata</i> (02-03)	1674.0	3.22	
DIA	<i>Aulacoseira islandica</i> morf. <i>helvetica</i> (99,02)	1676.0	3.22	
DIA	<i>Stephanodiscus alpinus</i>	1721.0	3.24	
DIA	<i>Aulacoseira islandica</i> morf. <i>helvetica</i> (98)	1763.8	3.25	
DIA	<i>Tabellaria flocculosa</i> (90-98)	1780.0	3.25	
CRY	<i>Cryptomonas erosa</i>	1803.0	3.26	
DIA	<i>Tabellaria flocculosa</i> (99-01,05)	1834.0	3.26	
DIA	<i>Tabellaria flocculosa</i> (03)	1867.0	3.27	
DIA	<i>Tabellaria flocculosa</i> (04)	1930.0	3.29	
DIA	<i>Tabellaria flocculosa</i> (02)	1968.0	3.29	
DIA	<i>Diatoma vulgare</i>	2000.0	3.30	
CRY	<i>Cryptomonas ovata</i> (04-05)	2108.0	3.32	>2048-4096 (3.6)
CRY	<i>Cryptomonas</i> sp.	2319.0	3.37	
CHR	<i>Mallomonas acaroides</i>	2358.0	3.37	
CHR	<i>Mallomonas</i> cfr. <i>acaroides</i>	2358.0	3.37	
CHLO	<i>Closterium aciculare</i> (85-02)	2375.0	3.38	
DIA	<i>Gomphonema truncatum</i>	2410.0	3.38	
CRY	Cfr. <i>Cryptomonas</i> sp. (99-04)	2482.0	3.39	
CRY	<i>Cryptomonas erosa</i> v. <i>reflexa</i> (88-89)	2500.0	3.40	
DIA	<i>Melosira varians</i>	2675.0	3.43	
CHR	<i>Mallomonas zellensis</i> (98-05)	2755.0	3.44	
CHLO	<i>Carteria</i> sp. (04)	2771.0	3.44	
DINO	<i>Peridinium inconspicuum</i>	2790.0	3.45	
CHLO	<i>Cosmarium bioculatum</i>	2984.0	3.47	
DIA	<i>Cyclotella bodanica</i>	2986.0	3.48	
DIA	<i>Cyclotella bodanica</i> var. <i>lemanica</i>	3022.0	3.48	
CHLO	<i>Staurastrum</i> sp.	3092.0	3.49	
CHR	<i>Mallomonas elongata</i> (98-05)	3183.0	3.50	
CHLO	<i>Closterium aciculare</i> (03-05)	3215.0	3.51	
CHR	<i>Mallomonas caudata</i> (84-89)	3489.0	3.54	
CHR	<i>Mallomonas</i> sp.	3489.0	3.54	
DINO	<i>Gymnodinium obesum</i>	3600.0	3.56	
DIA	<i>Synedra acus</i>	3678.0	3.57	
DIA	<i>Diatoma ehrenbergii</i>	4040.0	3.61	
CHR	<i>Mallomonas elongata</i> (92-94)	4059.0	3.61	
CHR	<i>Mallomonas zellensis</i> (90-97)	4059.0	3.61	

(continued)

**Tab. 2.** Continuation (page 6).

Taxonomic group	Operational Taxonomic Unit (OTU)	Cell Volume (V, $\mu\text{m}^3$ )	LogV	Size Class: The volume range and the upper border log
DIA	<i>Cyclotella bodanica</i> var. <i>bodanica</i>	4235.0	3.63	>4096-8192 (3.9)
CHLO	<i>Staurastrum gracile</i>	4662.0	3.67	
CHR	<i>Mallomonas elongata</i> (89)	5250.0	3.72	>8192-16384 (4.2)
DINO	<i>Gymnodinium</i> sp. (4)	5695.0	3.76	
CHR	<i>Mallomonas caudata</i> (05)	6120.0	3.79	>16384-32768 (4.5)
DIA	<i>Synedra ulna</i>	7500.0	3.88	
CHR	<i>Mallomonas caudata</i> (90-04)	8134.0	3.91	>32768-65536 (4.8)
DINO	<i>Peridinium aciculiferum</i>	8500.0	3.93	
DINO	<i>Gymnodinium uberrimum</i> (04)	8888.0	3.95	>65536-131072 (5.1)
DINO	<i>Gymnodinium uberrimum</i>	9687.0	3.99	
CHLO	<i>Staurastrum</i> cfr. <i>paradoxum</i>	9917.0	4.00	
CHLO	<i>Staurastrum pingue</i>	9917.0	4.00	
DINO	<i>Gymnodinium helveticum</i> (84-85)	11231.0	4.05	
DINO	<i>Gymnodinium helveticum</i> (87-05)	15494.0	4.19	
DIA	<i>Synedra ulna</i> var. <i>danica</i>	19262.0	4.28	
CHLO	<i>Cosmarium depressum</i>	24000.0	4.38	
DINO	<i>Gymnodinium</i> sp. (1)	26300.0	4.42	
DINO	<i>Gymnodinium helveticum</i> (86)	28283.0	4.45	
DINO	<i>Gymnodinium</i> sp. (3)	30954.0	4.49	
DINO	<i>Gymnodinium</i> sp. (2)	35608.0	4.55	
DINO	<i>Peridinium cinctum</i>	44799.0	4.65	
DINO	<i>Peridinium willei</i> (small)	59706.0	4.78	
DINO	<i>Ceratium hirundinella</i>	72282.0	4.86	
DINO	<i>Peridinium willei</i> (large)	85180.0	4.93	

Received: August 2008

Accepted: January 2009